



ELSEVIER

Journal of Alloys and Compounds 293–295 (1999) 648–652

Journal of  
ALLOYS  
AND COMPOUNDS

# Studies on the electrochemical properties of $\text{MNi}_{4.3-x}\text{Co}_x\text{Al}_{0.7}$ hydride alloy electrodes

Hongge Pan\*, Jianxin Ma, Chunsheng Wang, Shaoan Chen, Xinghua Wang, Changpin Chen, Qidong Wang

Department of Materials Science and Engineering, Zhejiang University, Hangzhou 310027, People's Republic of China

## Abstract

In this paper, the electrochemical properties of  $\text{MNi}_{4.3-x}\text{Co}_x\text{Al}_{0.7}$  electrode alloys, including high rate dischargeability, exchange current density  $I_0$ , limiting current density  $I_L$ , and diffusion coefficient of hydrogen in the hydride  $D_\alpha$  by means of linear polarization, anodic polarization, and electrochemical impedance spectroscopy were systematically studied. The results indicate that, with the increase of Co content, the cyclic stability is improved markedly, which agrees with previous investigation. However, activation becomes more difficult, and the high rate dischargeability decreases. The linear polarization and anodic polarization results suggest that the exchange current density  $I_0$  and limiting current density  $I_L$  decrease from the 395 ( $x=0$ ) to 33  $\text{mA g}^{-1}$  ( $x=1.3$ ) and from 2263 ( $x=0$ ) to 308  $\text{mA g}^{-1}$ , respectively. The electrochemical impedance spectroscopy result also reveals that the diffusion coefficient of hydrogen in the alloys decreases rapidly with the increase in Co content in  $\text{MNi}_{4.3-x}\text{Co}_x\text{Al}_{0.7}$  hydride alloy electrodes. © 1999 Elsevier Science S.A. All rights reserved.

**Keywords:** Electrochemical properties;  $\text{AB}_5$  type alloy; Hydrogen storage alloy electrode

## 1. Introduction

Nickel–metal hydride (Ni–MH) batteries have been extensively investigated and produced because of their high energy density, high charge and discharge rate ability, long cycle life, no dendrite formation, and environmental compatibility [1–3].

Two classes of metal hydride alloys currently being developed are  $\text{AB}_5$  type intermetallic compounds, where A represents rare earth elements and B includes any of late transition or p-shell elements [4,5], and  $\text{AB}_2$  type Laves phases, where A and B both denote early transition elements [6]. Although the  $\text{AB}_2$  alloys are reported to exhibit higher specific energy than that of  $\text{AB}_5$  alloys, state-of-the-art commercial Ni–MH batteries are predominately use  $\text{AB}_5$  alloys because of their better overall electrochemical properties.

Although  $\text{LaNi}_5$  alloys has a high absorption and desorption hydrogen capacity, easy electrochemical activation and good charge and discharge kinetics [7], the storage capacity of this alloy declines rapidly during

charge and discharge cyclings because the La on its surface is oxidized to  $\text{La}(\text{OH})_3$  easily. A breakthrough was made by Willems and Buschow [4] who found that partial substitution of Ni by Co was very effective to enhance the cycle life of  $\text{LaNi}_5$  alloy. Since then, many scientists have investigated the influence of Co on the cycle life of  $\text{LaNi}_5$  based alloys [8–15]. Up to now, cobalt has been thought to be indispensable for  $\text{AB}_5$  type battery electrodes. However, the effect of Co on the electrochemical properties rather than cycle life and activation has not been systematically investigated.

## 2. Experimental

Hydrogen storage alloys of nominal composition  $\text{MNi}_{4.3-x}\text{Co}_x\text{Al}_{0.7}$  ( $x=0.0, 0.5, 0.7, 0.9, 1.1, 1.3$ ) were prepared by arc melting under an argon atmosphere. The M1 stands for lanthanum-rich misch metal which composed of 80 wt% La, 10 wt% Ce, 6 wt% Pr, and 5 wt% Nd. The purity of the other metals is above 99.7%. Ingots were turned over and remelted five times for homogeneity during melting. The ingots were mechanically pulverized and ground into fined powders with an average size of 40  $\mu\text{m}$  for to be used as electrode materials.

\*Corresponding author. Tel.: +86-571-795-1406; fax: +86-571-795-1152.

E-mail address: pan\_hg@mail.hz.zj.en (H. Pan)

The metal hydride electrode was made by first mixing thoroughly 0.5 g of alloy powder with 0.2 g of carbonyl nickel powder, then 3% PVA solution was added to the mixture as binder. The mixture was cold pressed onto an Ni mesh under pressure of 20 MPa. The apparent surface area of the electrode was  $1.5 \times 1.5 \text{ cm}^2$  with a thickness of  $\approx 1.5 \text{ mm}$ . The electrode for the cyclic lifetime study was sandwiched with two Ni meshes to prevent stripping of the alloys [16].

The cell for electrochemical measurement consisted of a working electrode (metal hydride), a counterelectrode ( $\text{NiOOH}/\text{Ni}(\text{OH})_2$  electrode), and a reference electrode ( $\text{Hg}/\text{HgO}$ ). The  $\text{Hg}/\text{HgO}$  electrode was equipped with Luggin tube to reduce the IR drop in the polarization and electrochemical impedance spectroscopy measurements. The electrolyte was 6 M KOH solution and the temperature was controlled at  $25 \pm 1^\circ\text{C}$ . The discharge capacity of the electrode was determined by the galvanostatic method. The cutoff voltage for discharging was fixed at  $-600 \text{ mV}$  with respect to the  $\text{Hg}/\text{HgO}$  electrode. For activation and cyclic lifetime investigation, the electrode was charged and discharged at 50 mA. For polarization and electrochemical impedance spectroscopy measurements, the hydrogen storage alloy electrode was first activated completely (20 cycle) and then was charged and discharged to the 50% SOD. The average particle size of hydride electrode after activation was determined by scanning electron microscopy (SEM).

In this paper, the stability of hydrogen storage alloy electrode after 250 cycle number [ $S_{(250)}$ ] has been expressed in terms of the capacity ratio as follows:

$$S_{(250)} = \frac{C_{i(250)}}{C_{i(0)}} \times 100\% \quad (1)$$

### 3. Results and discussion

#### 3.1. Effect of Co content on the thermodynamic properties

Fig. 1 shows the activation characteristics of  $\text{MINi}_{4.3-x}\text{Co}_x\text{Al}_{0.7}$  hydride electrodes. The capacity of  $\text{MINi}_{4.3}\text{Al}_{0.7}$  hydride electrode decreases linearly with the cycle number. This can be attributed to the unstability of  $\text{MINi}_{4.3}\text{Al}_{0.7}$  hydride electrode in KOH solution and formatting to  $\text{La}(\text{OH})_3$  and nickel. The corrosion-resistance of the electrode increases rapidly with the Co content  $x$  increase from 0.0 to 0.5 in the  $\text{MINi}_{4.3-x}\text{Co}_x\text{Al}_{0.7}$  alloy electrodes, and the activation becomes rather difficult with the further increase of Co content.

The maximum capacities of the  $\text{MINi}_{4.3-x}\text{Co}_x\text{Al}_{0.7}$  hydride electrodes are listed in Table 1. It should be emphasized that the maximum capacities of the  $\text{MINi}_{4.3}\text{Al}_{0.7}$  and  $\text{MINi}_{4.0}\text{Co}_{0.3}\text{Al}_{0.7}$  hydride electrodes are the maximum capacities after corrosion. Their real capaci-

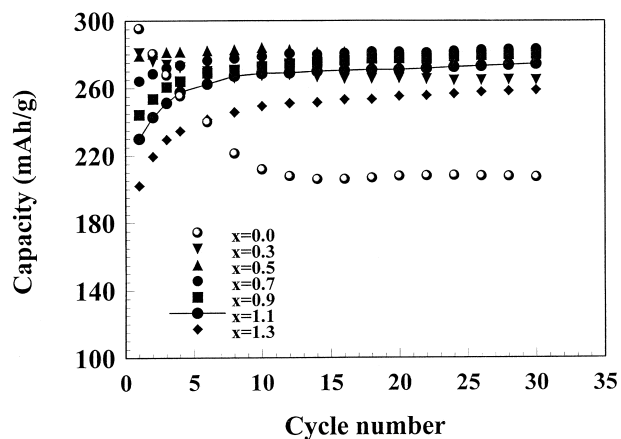


Fig. 1. Activation characteristics of the  $\text{MINi}_{4.3-x}\text{Co}_x\text{Al}_{0.7}$  hydride electrodes.

ties should be higher than those listed in Table 1. As can be seen from Table 1 the capacity of the hydride electrode decreases with the increasing Co content in the alloys, but this decrease is not very large.

The effect of Co content in the  $\text{MINi}_{4.3-x}\text{Co}_x\text{Al}_{0.7}$  alloys on the cycle life of  $\text{MINi}_{4.3-x}\text{Co}_x\text{Al}_{0.7}$  hydride electrodes are shown in Fig. 2. The corresponding parameter  $S_{(250)}$  are also listed in Table 1. The cycle life of hydride increases rapidly with the Co content from 0.0 to 0.7, but the improvement of cycle life becomes much less markedly with further increase of Co content.

#### 3.2. Effect of Co content on the kinetic properties

One main parameter for the practical application of hydride electrodes is the rate capacity, i.e. the amount of charge which can be recovered during galvanostatic discharge. The high rate dischargeability (HRD) is defined as the ratio of the discharge capacity  $Q_i$  at cutoff voltage 0.6 V at the discharge current density  $I_d$  to the maximum discharge capacity  $Q_{\max}$ .

$$\text{HRD} = (Q_i / Q_{\max}) \times 100\% \quad (2)$$

The high rate dischargeability is shown in Fig. 3. The HRD decreases with the increase of the Co content in the  $\text{MINi}_{4.3-x}\text{Co}_x\text{Al}_{0.7}$  hydride electrodes, especially for high discharge current density. Furthermore, the effect of Co content on the HRD when the values of  $x$  is between 0.0 and 0.7 is smaller than that when the values of  $x$  is large than 0.7. In a word, the higher the content of Co content in the  $\text{MINi}_{4.3-x}\text{Co}_x\text{Al}_{0.7}$  hydride electrodes, the lower the HRD.

After activation, the HRD or the kinetic properties of hydride electrodes were mainly determined by the exchange current density  $I_0$ , the diffusion coefficient of hydrogen in the  $\alpha$  phase  $D_\alpha$  or the limiting current density  $I_L$  [16].

Table 1

The capacity  $Q_{\max}$ , cyclic stability  $S_{(250)}$ , exchange current density  $I_0$ , limiting current density  $I_L$ , symmetry  $\beta$ , and the apparent diffusion coefficient of hydrogen  $D_\alpha$  in the  $\alpha$  phase in  $\text{MINi}_{4.3-x}\text{Co}_x\text{Al}_{0.7}$  hydride electrodes

Values of $x$ in $\text{MINi}_{4.3-x}\text{Co}_x\text{Al}_{0.7}$	$Q_{\max}$ (mA h g <sup>-1</sup> )	$S_{(250)}$	$I_0$ (mA g <sup>-1</sup> )	$I_L$ (mA g <sup>-1</sup> )	$\beta$	$D_\alpha$ (cm <sup>2</sup> s <sup>-1</sup> )
0.0	295	6.4	395	2263	0.85	$1.4 \times 10^{-9}$
0.3	301	14.8	233	1295	0.74	$9.8 \times 10^{-10}$
0.5	292	44.9	147	1053	0.67	$8.1 \times 10^{-10}$
0.7	285	63.6	91	805	0.64	$5.4 \times 10^{-10}$
0.9	280	76.0	75	477	0.61	$4.1 \times 10^{-10}$
1.1	271	85.3	45	390	0.57	$3.2 \times 10^{-10}$
1.3	260	86.5	33	308	0.43	$2.1 \times 10^{-10}$

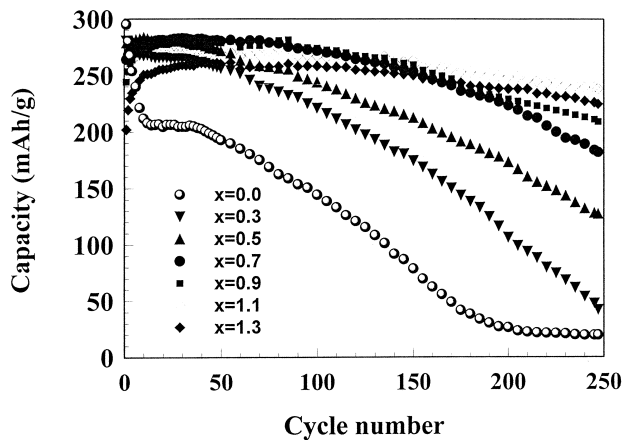


Fig. 2. Cycle life of the  $\text{MINi}_{4.3-x}\text{Co}_x\text{Al}_{0.7}$  hydride electrodes.

In order to determine the exchange current density  $I_0$  and the polarization resistance, the linear polarization experiment was conducted at 50% SOD and scanning rate of  $5 \text{ mV s}^{-1}$ . The results are presented in Fig. 4, which reveals that the polarization increases with the increase in Co content in the  $\text{MINi}_{4.3-x}\text{Co}_x\text{Al}_{0.7}$  hydride electrodes. The exchange current density  $I_0$  can be calculated according to the following formula [17]:

$$I_0 = \frac{I_d RT}{F \eta} \quad (3)$$

where  $F$ ,  $R$ , and  $T$  are the Faraday constant, the gas constant, and absolute temperature, respectively, and  $\eta$  is the total polarization at the discharge current density  $I_d$ .

The exchange current density  $I_0$  calculated by Eq. (3) are listed in Table 1. The exchange current density  $I_0$  decreases from  $395 \text{ mA g}^{-1}$  for  $x=0.0$  to  $33 \text{ mA g}^{-1}$  for  $x=1.3$ , respectively. This means that, with the increase in Co content  $x$ , the  $I_0$  decreases seriously.

During galvanostatic discharge, the apparent diffusion coefficient of hydrogen in  $\alpha$  phase (including hydrogen diffusion through the oxidation film on the surface of particles) can be calculated by the equation followed [18]:

$$D_\alpha = \frac{r_0^2 I_d}{15(Q_0 - \tau I_d)} \quad (4)$$

Where  $Q_0$ ,  $I_d$ ,  $\tau$ , and  $r_0$  is the initial specific capacity, the discharge current density, transition time, i.e. the time when the hydrogen surface concentration is zero, and the average particle radius, respectively.

The calculated values of  $D_\alpha$  according to Eq. (4) are also presented in Table 1. Fig. 5 shows the relationship of  $D_\alpha$  with the Co content. It can be seen that the apparent

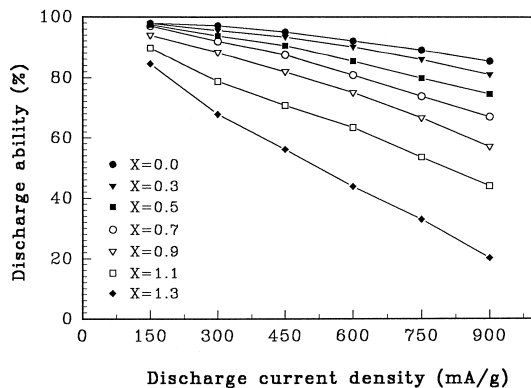


Fig. 3. High rate dischargeability HRD of the  $\text{MINi}_{4.3-x}\text{Co}_x\text{Al}_{0.7}$  hydride electrodes.

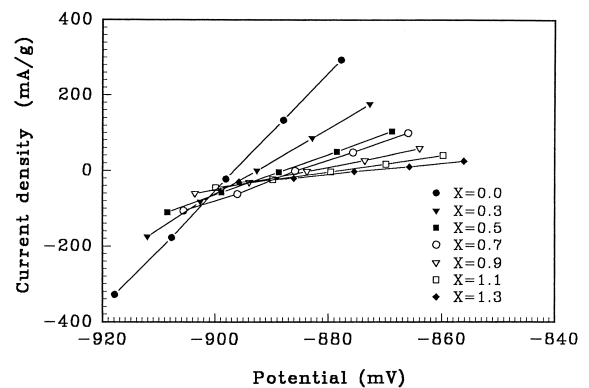


Fig. 4. Linear polarization curves of the  $\text{MINi}_{4.3-x}\text{Co}_x\text{Al}_{0.7}$  hydride electrodes.

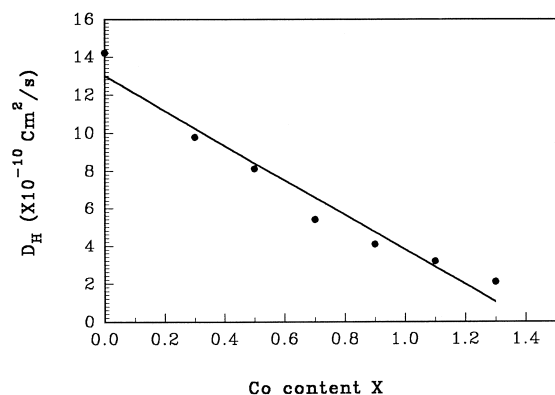


Fig. 5. Relationship between  $D_\alpha$  and Co content in the  $\text{MINi}_{4.3-x}\text{Co}_x\text{Al}_{0.7}$  hydride electrodes.

diffusion coefficient of hydrogen in the  $\alpha$  phase  $D_\alpha$  is almost inversely proportional to the Co content in the  $\text{MINi}_{4.3-x}\text{Co}_x\text{Al}_{0.7}$  hydride electrodes. The apparent diffusion coefficient of hydrogen in  $\alpha$  phase  $D_\alpha$  decreases with the increase in Co content. For example, the  $D_\alpha$  at  $x=0.0$  is nine times higher than that at  $x=1.3$ . This result also can be confirmed by the results of electrochemical impedance spectra. Fig. 6 shows the electrochemical impedance spectra of in the  $\text{MINi}_{4.3-x}\text{Co}_x\text{Al}_{0.7}$  hydride electrodes at  $x=0.3, 0.7, 0.9, 1.1,$  and  $1.3$ . According to Wang's mathematical model [19], the low frequency semicircle in the electrochemical impedance spectra is attributed to the hydrogen diffusion in the  $\alpha$  phase. The radius of this semicircle increases with increasing Co content means that the apparent diffusion coefficient of hydrogen in  $\alpha$  phase  $D_\alpha$  decreases with the increase of Co content  $x$  in  $\text{MINi}_{4.3-x}\text{Co}_x\text{Al}_{0.7}$  hydride electrodes.

Fig. 7 shows that the anodic current density in response to the overpotential of the  $\text{MINi}_{4.3-x}\text{Co}_x\text{Al}_{0.7}$  hydride electrodes at 50% SOD. The total overpotential at same discharge current density increases with increasing Co content  $x$ . The corresponding limiting current density  $I_L$  at different values of  $x$  is listed in Table 1. The limiting

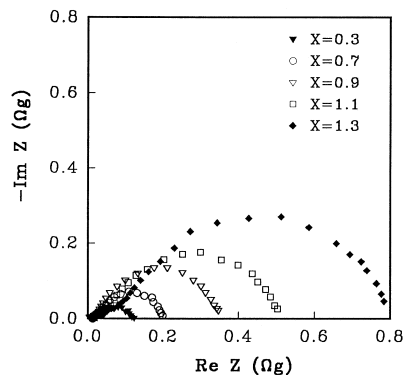


Fig. 6. Electrochemical impedance spectra of the  $\text{MINi}_{4.3-x}\text{Co}_x\text{Al}_{0.7}$  hydride electrodes at  $x=0.3, 0.7, 0.9, 1.1,$  and  $1.3$ .

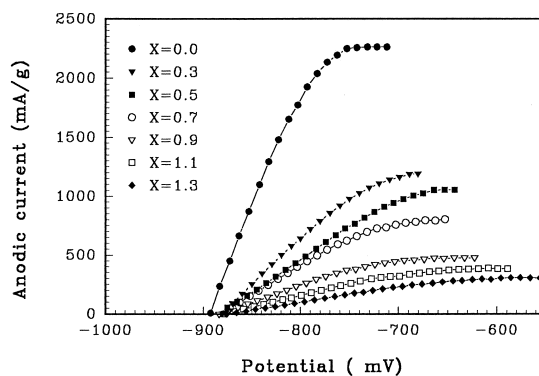


Fig. 7. Anodic polarization of the  $\text{MINi}_{4.3-x}\text{Co}_x\text{Al}_{0.7}$  hydride electrodes.

current density  $I_L$  decreases dramatically with the increase in  $x$ , i.e. the limiting current density  $I_L$  at  $x=0.0$  is about eight times higher compared with that at  $x=1.3$  in the  $\text{MINi}_{4.3-x}\text{Co}_x\text{Al}_{0.7}$  hydride electrodes.

The overpotential of anodic polarization can be expressed as [20]:

$$\eta = \frac{RT}{\beta F} \ln\left(\frac{I_L}{I_0}\right) + \frac{RT}{\beta F} \ln\left(\frac{I_d}{I_L - I_d}\right) \quad (5)$$

According to Eq. (5), a plot of  $\eta$  vs.  $\ln(I_d/I_L - I_d)$  should be a straight line with  $RT/\beta F$  as its slope. Therefore, symmetry factor in the oxidation direction can be calculated from data of  $I_L$  and  $T$ . The calculated  $\beta$  is also listed in Table 1. It can be seen that the symmetry factor in the oxidation direction  $\beta$  decreases with increasing Co content  $x$ .

#### 4. Conclusions

In this paper, the effect of Co content on the thermodynamic and kinetic properties of the  $\text{MINi}_{4.3-x}\text{Co}_x\text{Al}_{0.7}$  hydride electrodes have been systematically studied. The results show that, with an increase of Co content, the cyclic stability is improved markedly, the activation becomes more difficult, and the high rate dischargeability decreases. The linear polarization and anodic polarization results indicate that the exchange current density  $I_0$  and limiting current density  $I_L$  decrease from the 395 ( $x=0$ ) to 33  $\text{mA g}^{-1}$  ( $x=1.3$ ) and from 2263 ( $x=0$ ) to 308  $\text{mA g}^{-1}$  in the  $\text{MINi}_{4.3-x}\text{Co}_x\text{Al}_{0.7}$  electrode alloys, respectively. The electrochemical impedance spectroscopy result also reveals that the diffusion coefficient of hydrogen in the alloys is much lower than that for  $x=0$  in the alloy.

#### Acknowledgements

This project was supported by National Natural Foundation of China under contract No. 59701005 and National 863 plan.

## References

- [1] T. Sakai, H. Miyamura, N. Kuriyama, A. Kato, K. Oguro, H. Ishikawa, *J. Electrochem. Soc.* 137 (1990) 795.
- [2] W. Zhang, M.P.S. Kumar, S. Srinivasan, *J. Electrochem. Soc.* 142 (1995) 2935.
- [3] T. Sakai, T. Iwaki, Z. Ye, J. Noreus, *J. Electrochem. Soc.* 142 (1995) 4040.
- [4] J.J.G. Willems, *Philips J. Res.* 39 (Suppl. 1) (1984) 1.
- [5] J.J.G. Willems, K.H.J. Buschow, *J. Less-Common Met.* 129 (1987) 13.
- [6] M.A. Feteenko, S. Venkatesan, K.C. Hong, B. Reichman (Eds.), *Proc. 16th Int. Power Source Symp.*, Vol. vol. 12, International Power Source Committee, UK, 1983, p. 411.
- [7] J.J.G. Van Beek J.R.G.C.M. Willems, H.C. Donkersloot, *Proc. 14th Power Source Symp.*, Brighton, in: L.J. Pearce (Ed.), *Power Sources*, Vol. 10, 1985, p. 317.
- [8] T. Sakai, H. Miyamura, N. Kuriyama, A. Kato, K. Oguro, H. Ishikawa, C. Iwakura, *J. Less-Common Met.* 159 (1990) 127.
- [9] T. Sakai, K. Oguro, H. Miyamura, N. Kuriyama, A. Kato, H. Ishikawa, C. Iwakura, *J. Less-Common Met.* 161 (1990) 193.
- [10] T. Sakai, T. Hazama, H. Miyamura, N. Kuriyama, A. Kato, H. Ishikawa, *J. Less-Common Met.* 172–174 (1991) 1175.
- [11] T. Sakai, H. Yoshinaga, H. Miyama, N. Kuriyama, H. Ishikawa, *J. Alloys Compd.* 180 (1992) 3.
- [12] M.P.S. Kumar, W. Zhang, K. Petrov, A. Rostami, S. Srinivasan, G.D. Adzic, J.J. Reilly, H.S. Lim, *J. Electrochem. Soc.* 142 (1995) 3424.
- [13] D. Chartouni, F. Meli, A. Zuttel, K. Gross, L. Schlapbach, *J. Alloys Compd.* 241 (1996) 160.
- [14] J.M. Cocciantlia, P. Berenard, S. Ferenandez, J. Atlin, *J. Alloys Compd.* 253–254 (1997) 642.
- [15] G.D. Adzic, J.R. Johnson, S. Mukerjee, J. McBreen, J.J. Reily, *J. Alloys Compd.* 253–254 (1997) 579.
- [16] C.S. Wang, Y. Q. Lei and Q. D. Wang, *Electrochim. Acta* (accepted for publication).
- [17] P.H.L. Notten, P. Hokkeling, *J. Electrochem. Soc.* 138 (1991) 1877.
- [18] G. Zheng, B.N. Popov, R.E. White, *J. Electrochem. Soc.* 142 (1995) 2695.
- [19] W. Chunsheng, *J. Electrochem. Soc.* 145 (1998) 1801.
- [20] H.W. Yang, Y.Y. Wang, C.C. Wan, *J. Electrochem. Soc.* 143 (1996) 429.